6522 *Biochemistry* **2009,** *48,* 6522–6531
DOI: 10.1021/bi900343n

BIOCHEMISTRY
including biophysical chemistry & molecular biology
Article

Protective Effects of L- and D-Carnosine on α-Crystallin Amyloid Fibril Formation: Implications for Cataract Disease†

Francesco Attanasio,‡ Sebastiano Cataldo,§ Salvatore Fisichella,∥ Silvia Nicoletti,∥ Vincenzo Giuseppe Nicoletti,∥,⊥ Bruno Pignataro,§ Anna Savarino,∥ and Enrico Rizzarelli*,∥

‡*Institute of Biostructures and Bioimaging (IBB), CNR, 95125 Catania, Italy,* §*Dipartimento di Chimica Fisica "F. Accascina", Università di Palermo, 90128 Palermo, Italy,* ∥*Department of Chemical Sciences, University of Catania, 95125 Catania, Italy, and* ⊥*National Institute of Biostructures and Biosystems, 95125 Catania, Italy*

Received February 27, 2009; Revised Manuscript Received May 14, 2009

ABSTRACT: Mildly denaturing conditions induce bovine α-crystallin, the major structural lens protein, to self-assemble into fibrillar structures in vitro. The natural dipeptide L-carnosine has been shown to have potential protective and therapeutic significance in many diseases. Carnosine derivatives have been proposed as potent agents for ophthalmic therapies of senile cataracts and diabetic ocular complications. Here we report the inhibitory effect induced by the peptide (L- and D-enantiomeric form) on α-crystallin fibrillation and the almost complete restoration of the chaperone activity lost after denaturant and/or heat stress. Scanning force microscopy (SFM), thioflavin T, and a turbidimetry assay have been used to determine the morphology of α-crystallin aggregates in the presence and absence of carnosine. DSC and a near-UV CD assay evidenced that the structural precursors of amyloid fibrils are polypeptide chain segments that lack stable structural elements. Moreover, we have found a disassembling effect of carnosine on α-crystallin amyloid fibrils. Finally, we show the ability of carnosine to restore most of the lens transparency in organ-cultured rat lenses exposed to similar denaturing conditions that were used for the in vitro experiments.

The internal composition of the ocular lens is dominated by a group of three structural proteins (*1*), namely, α-, *β*-, and *γ*-crystallins. α-Crystallin is the major structural lens protein and belongs to the heat shock protein family. It acts as a molecular chaperone, thus being crucial in protecting various proteins against aggregation induced by heating, chaotropic agents, reduction, and chemical modification (*2*−*5*).

In its native state, α-crystallin consists of two closely related subunits, αA and αB, each being ∼20 kDa, and it is present in the form of a large, heterogeneous, water-soluble aggregate (molecular mass of ∼800 kDa) (*6*). In aged lenses, the appearance of high-molecular mass aggregates (more than 1000 kDa) and insoluble proteins has been observed (*7*, *8*).

Protein aggregation can proceed via a disordered mechanism, such as irregular and amorphous aggregation, or an ordered mechanism, associated with amyloid fibril formation featured by intermolecular *β*-sheet structure (*9*). Post-translational modifications of lens crystallins may result in conformational changes and aggregation, leading to lens opacification and cataract formation (*10*). Two possible mechanisms have been proposed for cataract formation: (i) a condensation phenomenon, in which lens opacification results from the loss of solubility of the crystallins (*11*); and (ii) a conformational disorder in which unfolding or destabilization of the crystallin proteins drives the aggregation (*12*). Neither fibrils nor filaments are observed in normal lenses (*13*, *14*), but under mildly denaturing conditions, bovine α-crystallin has been shown to assemble into fibrillar structures in vitro. Thus, the tendency of the crystallins to convert into fibrils under destabilizing conditions suggests that this process could contribute to the development of cataract with aging.

Cataract is a relevant cause of vision impairment, and surgical replacement of the lens actually represents the only treatment available. Several small molecules able to counteract this conformational protein disease have been studied with the perspective of developing new therapeutic interventions (*15*−*20*).

The endogenous histidine-bearing dipeptide, L-carnosine (*β*-alanyl-L-histidine), is present in long-lived tissues in large amounts and has been shown to delay aging of cultured cell, and to have potential biochemical and therapeutic significance (*19*, *21*−*25*). In addition, these carnosine features can be extended to the protection against inactivation of enzymes induced by glycation, oxidation, and steroids (*26*−*28*), and protection of neural cells from malondialdehyde-induced toxicity (*29*). Finally, carnosine derivatives exhibit efficacy in the direct intervention of treating cataract (*30*, *31*).

L-Carnosine is, however, known to be rapidly hydrolyzed in human serum by specific hydrolytic enzymes (carnosinases), which limit its possible therapeutic uses (*32*). Such a problem can be solved by the use of D-carnosine, the non-natural isomer, which is resistant to hydrolysis by carnosinases, it being so stable

†This research was supported by MIUR.
*To whom correspondence should be addressed. E-mail: erizzarelli@unict.it. Telephone: +390957385070. Fax: +39095337678.

 Published on Web 05/14/2009

in the plasma and able to cross the blood−brain barrier and, therefore, suitable for systemic interventions in protein misfolding-related diseases (*33*).

In this study, we have investigated the ability of L- and D-carnosine to counteract α-crystallin amyloid fibril formation under destabilizing conditions and demonstrated that their protective role against fibrillogenesis not only is preventive but also can disrupt already formed fibrils. Moreover, such effects can be extended to the entire lens maintained in organ cultures. Indeed, carnosine has shown either to prevent or to recover the lens opacification under denaturing conditions.

MATERIALS AND METHODS

Chemicals. α- and β-crystallin, M-199 (TC 199) culture medium, antibiotic solution, and all chemicals for buffer salts were purchased from Sigma Chemical Co. (St. Louis, MO). L-Carnosine was purchased from Fluka (batch 22030); D-carnosine was provided by Flamma s.p.a. (Bergamo, Italy).

Formation of Amyloid Fibrils by Bovine α-Crystallin. Bovine α-crystallin (10 mg/mL) was dissolved in 0.1 M phosphate buffer and 1 M guanidine HCl (pH 7.2) alone or in the presence of 0.1 M carnosine, and the samples were incubated at 60 °C for 24 h. According to Meehan et al. (*13*), these are the required conditions for generating fibril assembly of α-crystallin in vitro within 24 h.

Scanning Force Microscopy. SFM[1] imaging was performed using a Multimode/Nanoscope IIIA instrument (Digital Instrument, Santa Barbara, CA). Protein samples (10 μL, 0.5 mg/mL) were deposited on freshly cleaved mica for 30 s, rinsed with ultrapure Milli-Q water, and dried with a dry nitrogen steam.

Moreover, carnosine (0.1 M) was added to the protein sample treated at 60 °C for 24 h in 1 M guanidine HCl to study its effect on the morphology of α-crystallin fibrils.

Commercially available etched silicon probes (Digital) were used, and 512 × 512 points were collected for each image by maintaining the scan rate at ~1 Hz.

To prevent protein damage, the instrument was set in dynamic mode working in the net tip−sample attractive regime, as previously described (*34*, *35*). Such a method showed unprecedented results in the scanning probe investigation area, especially as far as it concerns the image quality and height values of biological systems. To evaluate the aggregation dimension of the building units (see below), we based them on height data. This because it is well-known that the SFM lateral investigation of nanostructures is affected by the so-called tip broadening effect (*36*). Accordingly, tip convolution effects leading to broadening of >10 nm are typically observed by conventional SFM probes for structures, like proteins, that are a few nanometers in size (*34*).

The following algorithm can be used to evaluate the extent of tip broadening (*37*): $W_{obs} = 4\sqrt{\frac{W}{2}R_{tip}}$ where W is the real width, W_{obs} the observed structure width, and R_{tip} the tip radius. Particle heights were measured by using the Nanoscope software and then gathered inside single data sets and statistically elaborated with Origin 8. A distribution histogram has been obtained by collecting hundreds of elements.

Sample Preparation for SFM. A 10 μL aliquot was removed from α-crystallin amyloid fibril solutions prepared as shown above (formation of amyloid fibrils) and diluted 200-fold into buffer. Moreover, L and D-carnosine were added to two aliquots removed from the fibril solution to study their time-dependent effect on the morphology. Also in that case, a 10 μL aliquot was removed from solutions and diluted 200-fold.

Calorimetric Assays. Differential scanning calorimetry (DSC) is a powerful technique for characterizing temperature-induced conformational changes in protein and other biological macromolecules. Calorimetric measurements were taken on a VP-DSC microcalorimeter (MicroCal Inc., Northampton, MA). All measurements were performed in 0.1 M phosphate buffer and 1 M guanidine HCl (pH 7.2). The protein and carnosine concentrations were 1.0 mg/mL and 0.1 M, respectively. The scan rate was 60 °C/h for all experiments. Reversibility of the unfolding transition was estimated by scanning the samples four times after cooling. All protein solutions were degassed at 20 °C before calorimetric measurements. Data analysis was performed using Origin (MicroCal).

CD Measurements. The CD spectrum of α-crystallin samples (1 mg/mL) was recorded at 25 and 60 °C on a Jasco (Tokyo, Japan) J-810 spectropolarimeter, thermostated with a Grant LTC 12-50 refrigerated circulating bath, processed by Jasco Spectra Manager 1.5, and corrected by subtraction of the background solvent spectrum obtained under identical experimental conditions. The CD spectrum was smoothed for clarity of display, made in triplicate, and acquired using a quartz cell with a path length of 10 mm for the near-UV range. All the data were converted to give specific ellipticity values (ψ) based on the sample concentration and expressed in degrees square centimeters per decagram. The α-crystallin concentration was determined spectrophotometrically by measuring the absorbance at 280 nm and using an extinction coefficient ε of 0.83.

ThT Fluorescence Measurements. Fluorescence emission spectra of ThT undergo a red shift upon incorporation into β-sheet amyloid structures (*38*, *39*). Aliquots of α-crystallin from incubated samples were added to the ThT solution in 0.1 M phosphate buffer (pH 7.2). Final solutions resulted in 50 μM ThT and contained 0.05 mg/mL protein. The measurements were taken using a Perkin-Elmer LS55 spectrofluorimeter.

Fluorescence emission spectra were monitored from 450 to 600 nm in a quartz cell with a light path of 1 cm. An excitation wavelength of 440 nm was used. Both excitation and emission bandwidths were set to 5 nm. The ThT spectra were corrected by subtraction of the background solvent spectrum obtained under identical experimental conditions. Ten consecutive spectra were recorded and merged; the experiments were performed in triplicate.

Chaperone Activity. Chaperone activities of native α-crystallin (0.25 mg/mL) and different α-crystallin fibrils, generated after thermal and chemical stress, were determined by their ability to prevent the increase in turbidity upon heating solutions of β_L-crystallin as described previously (*2*). This is the most widely used method for chaperone function in the α-crystallin field.

Bovine β_L-crystallin (0.5 mg/mL) was dissolved in 0.1 M phosphate buffer, and its aggregation was monitored at 55 °C in a diode-array Agilent (Santa Clara, CA) 8453 spectrophotometer equipped with a thermostatic cell holder and a Thermo-Haake C40P programmable refrigerated circulating bath. The change in light scattering and/or turbidity was monitored by measuring the absorbance at a wavelength of 400 nm as a

[1]Abbreviations: SFM, scanning force microscopy; DSC, differential scanning calorimetry; C_p, heat capacity; CD, circular dichroism; ThT, thioflavin T; HEPES, 4-(2-hydroxyethyl)piperazine-1-ethanesulfonic acid.

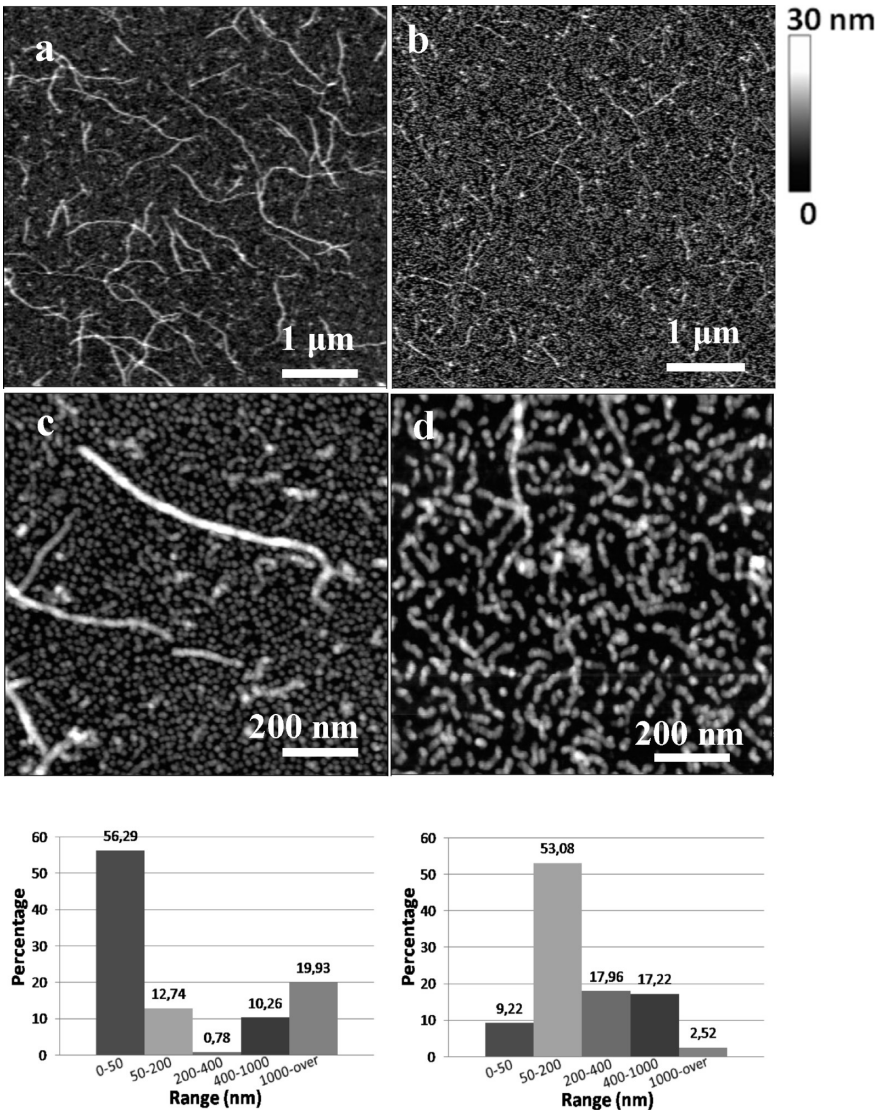

FIGURE 1: SFM images of 10 mg/mL α-crystallin co-incubated at 60 °C for 24 h with (a and c) 1 M guanidine and (b and d) 1 M guanidine and 0.1 M D-carnosine and relative statistical distributions of globular structure building units shown in the images.

function of time. Assays were performed using a quartz cell with a path length of 1 cm. The ratio of β_L-crystallin to α-crystallin was 2:1 for each experiment.

Rat Lens Organ Cultures. (i) Lens Extraction. Lenses were extracted through a posterior approach from the eyes of 1-month-old *Rattus norvegicus* (female, Sprague-Dawley) killed in a CO_2 gas chamber, taking particular care to guarantee minimal contamination by other ocular tissues and mechanical damage. Rats used for the study were obtained from the animal house stock of the host department and handled in accordance with the guidelines as per the host's Institutional Animal Ethical Committee.

(ii) Culture Conditions. Rat lenses were organ cultured in protein-free M-199 medium (with HEPES buffer), 100 units/mL penicillin, and 0.1 mg/mL streptomycin, under 5% CO_2 at 37 °C in the humidified environment of a cell culture incubator. Guanidine and L-carnosine were prepared by dissolving each compound in the medium to give a final concentration of 1 M as a stock solution. After 24 h, lenses were checked, and those developing eventual opacification due to mechanical damaging during extraction were discarded. Lenses were maintained in a 24-well culture plate with 2 mL of medium/well and one or two lenses per well for the period required.

RESULTS

Carnosine Inhibits α-Crystallin Fibrillation. In its native state, α-crystallin self-assembles into roughly spherical aggregates (*20*, *40*), whereas under destabilizing conditions, fibril assembly can be obtained (*13*).

Figure 1 shows the inhibition effect induced by carnosine on α-crystallin fibrillation. In particular, Figure 1a shows the SFM image of the control sample (1 M guanidine, 60 °C, 24 h), resulting in the formation of a mixture of structures, including globular systems on average 2.6 nm tall and 20−50 nm wide as well as fibril structures 12−20 nm tall and from hundreds of nanometers to a few micrometers long. Note that the fibril structures appear typically as linear aggregates closely resembling rows of beads, i.e., consisting of the self-aggregation of globular systems. Figure 1b shows the SFM image of the α-crystallin sample co-incubated in 0.1 M D-carnosine (1 M guanidine, 60 °C, 24 h), the inhibition of the formation of large fibers being clearly observed. In panels c and d of Figure 1, zoom-in images obtained in restricted regions of panels a and b of Figure 1, respectively, are shown. The SFM data were then analyzed quantitatively to evaluate the portion of proteins involved in the aggregation process, and the statistical analysis is also reported in Figure 1.

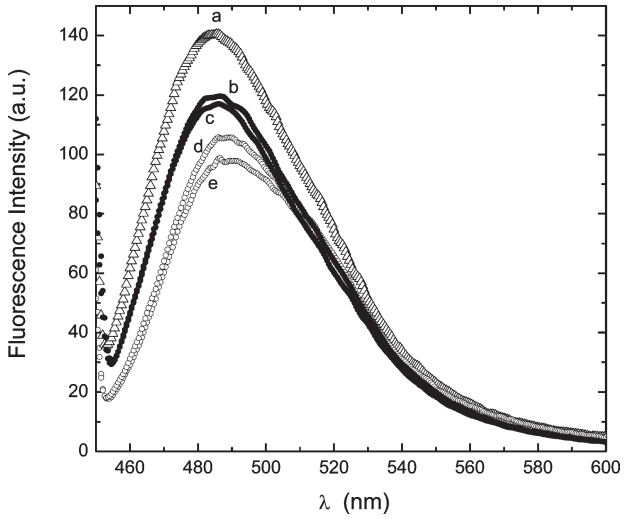

FIGURE 2: Assay of the effect of D- and L-carnosine on α-crystallin amyloid fibrils. (a) ThT fluorescence spectra of α-crystallin in 1 M guanidine incubated at 60 °C for 24 h. (b and c) ThT fluorescence spectra of α-crystallin in 1 M guanidine co-incubated with D- and L-carnosine, respectively, at 60 °C for 24 h. (d and e) ThT fluorescence spectra of a sample of α-crystallin in 1 M guanidine, incubated at 60 °C for 24 h, after treatment for 5 h with D- and L-carnosine, respectively.

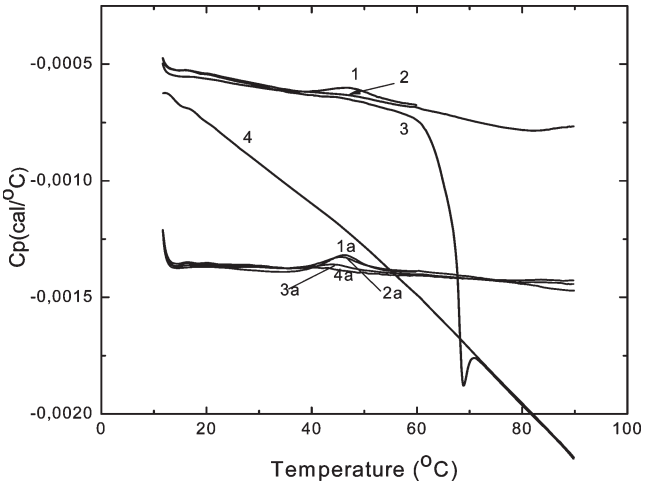

FIGURE 3: DSC profiles of the temperature dependencies of the heat capacity for four consecutive scans of α-crystallin (1 mg/mL) in 1 M guanidine (curves 1−4) and in 1 M guanidine with 0.1 M L-carnosine (curves 1a−4a), in 0.1 M phosphate buffer (pH 7.2) with a scan rate of 60 °C/h and a scan range of 10−90 °C.

The relative histograms have been obtained assuming the aggregation mechanism proposed for other similar systems (*41*) by considering the fibrils as a row of beads (see above) and as building units, with the smallest globular systems observed at the surface which were 2.6 nm in diameter. The amount of building units within each structure has been calculated in the reported dimensional ranges. In the control sample (Figure 1a), ∼20% of building units are involved in the formation of fibrils longer than 1000 nm, ∼11% constitute fibrils in the 200−1000 nm range, and 13 and 56% would form shorter fibrils (50−200 nm long) along with low-weight globular aggregates (0−50 nm). As a result of the co-incubation with 0.1 M D-carnosine (Figure1b), ∼53% of the building units give rise to the formation of 50−200 nm fibrils, whereas ∼10% result in nanoscopic globular structures (0−50 nm) and 35% in fibrils not exceeding 1000 nm in length. Only 2% of the building units are involved in the formation of fibrils longer than 1000 nm. Similar results have been found in the case of L-carnosine (data not shown).

According to the decrease of the fibrillar structures in SFM images, a lower ThT fluorescence intensity was recorded in the samples containing D- and L-carnosine co-incubated with α-crystallin under destabilizing conditions [Figure 2 (●), curves b and c] with respect to the control (curve a), indicating a reduction in the level of β-amyloid structures.

Effects of Carnosine on the Thermal Unfolding and Refolding of α-Crystallin. The above inhibitory effects are in principle expected to be related to the folding state of α-crystallin in the presence of carnosine. To investigate this aspect, we performed both DSC and near-UV CD experiments.

Given the remarkable stability of α-crystallin within the lens, the propensity of the protein aggregates to assemble into amyloid fibrils is likely increased as a result of factors that cause destabilization. It is noteworthy that temperature and/or chaotropic agents such as urea and guanidine hydrochloride destabilize macromolecular structures (*42*, *43*).

DSC measures the heat changes associated with thermal denaturation of biomolecules. Four consecutive heating scans are represented in Figure 3. DSC profiles showed that either in the presence of 1 M guanidine (curve 1) or in the presence of 1 M guanidine and 0.1 M L-carnosine (curve 1a) the endothermic peak of α-crystallin (T_m), corresponding to protein unfolding, shifted from 62.2 (*19*) to 46.3 °C, indicating the destabilization of the native form of the protein in the presence of guanidine. After the samples had cooled from the first run, the subsequent thermograms showed different traces for the two samples; in particular, for the sample containing protein and guanidine alone, the endothermic peak disappears (Figure 4, curve 2), probably due to the irreversible aggregation of the native proteins. An exothermic effect appears after 60 °C that became prominent in the third and fourth scans (Figure 4, curves 3 and 4) where a remarkable negative change in the Cp trace over the temperature range scanned was present, indicating the generation of different aggregated species.

In contrast, the thermograms of the same samples with L-carnosine exhibit in the second consecutive run (Figure 4, curve 2a) a relatively similar Cp trace with respect to the first one (Figure 4, curve 1a), indicating a reversible folding-unfolding transition in the presence of L-carnosine. Finally, in the third and fourth scans (Figure 4, curves 3a and 4a), no abrupt decrease in the Cp trace over the temperature range was present, suggesting a protection effect of L-carnosine on the generation of aggregated species. The same effects were observed in the presence of D-carnosine (data not shown).

The changes in the near-UV CD spectra of α-crystallin upon thermal unfolding reflect modifications in the local environment of aromatic residues. Spectra of different α-crystallin samples are presented in Figure 4. At 25 °C, the native α-crystallin spectrum (Figure 4a, curve 1) was similar to those of previous reports (*44*): the minimum at 291 nm and, coupled to it, that at 282 nm arise from tryptophan residues, and the transitions below 267 nm are characteristic of phenylalanine structures (*45*). The remaining transitions between 267 and 291 nm arise from tyrosine and/or tryptophan (*46*).

In the sample containing 1 M guanidine (Figure 4b, curve 1) or 1 M guanidine with 0.1 M L-carnosine (Figure 4c, curve 1), the peak intensity mildly decreased: the phenylalanine maxima and tryptophan minimum were practically unaffected, but changes

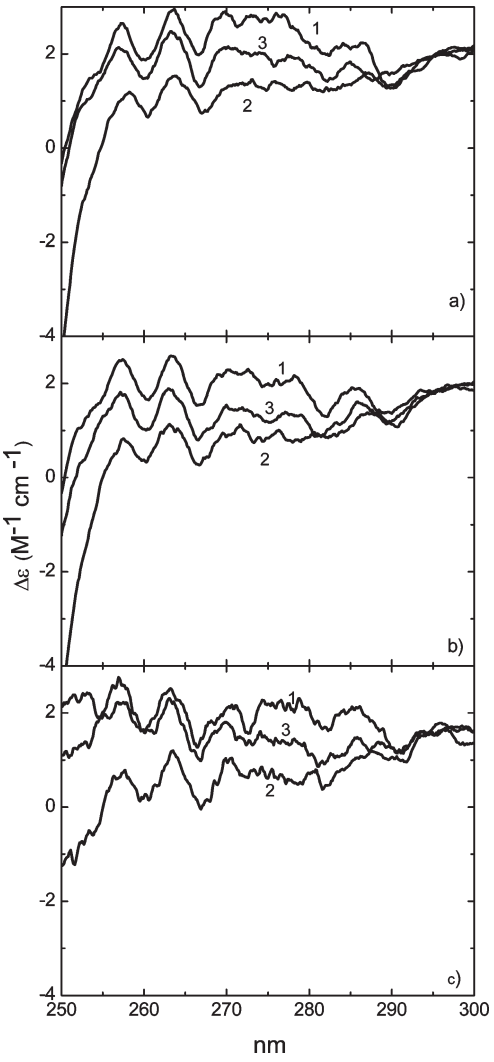

FIGURE 4: Near-UV CD spectra of (a) α-crystallin, (b) α-crystallin in 1 M guanidine, and (c) α-crystallin in 1 M guanidine and 0.1 M L-carnosine recorded at 25 °C (curve 1), at 60 °C (curve 2), and then again at 25 °C (curve 3).

were present in the tyrosine and tryptophan peaks between 267 and 291 nm.

The spectra at 60 °C were similar for all samples (Figure 4a−c, curves 1−3): with respect to the spectra at 25 °C, they showed a lack of any fine structure above 270 nm and the persistence of the two phenylalanine peaks below 270 nm. Cooling the sample at 25 °C did not restore all the peaks to their original intensity: in particular, only the spectrum of the sample containing 0.1 M L-carnosine (Figure 4c, curve 3) recovered the original intensity after thermal stress; for the other spectra, especially in the peaks between 267 and 291 nm, the observed restoration was partial and, for the sample in 1 M guanidine, rather weak (panels a and b of Figure 4, respectively, curve 3).

Carnosine Dissolves α-Crystallin Fibrils. We performed a variety of experiments to determine whether carnosine could dissolve existing α-crystallin fibrils. The addition of either D- or L-carnosine (0.1 M) to the sample with a consistent number of fibrillar structures showed a decrease in ThT fluorescence [Figure 2 (○), curves d and e] with respect to the control (curve a), suggesting that both carnosines promoted disassembly.

To investigate in more detail the disassembly process, SFM studies were conducted. The SFM images (Figure 5) showed that, after treatment for 1 h with D-carnosine (Figure 5a) and L-carnosine (Figure 5b), only a small amount of long fibrils (from 200 to > 1000 nm) is observed (10−15% of building units), the largest amount of proteins being present in the form of short fibrils (55−60%) and globular structures (25−30%). The histograms in panels a and b of Figure 5 are representative of the disassembly process by D- and L-carnosine, respectively. In Figure 5c−e, SFM images of some representative short fibrils after treatment with L-carnosine for 1, 3, and 5 h, respectively, are reported. Note that, with an increase in incubation time, the flexibility of fibrils tends to increase. This process was accompanied by dismantling of the fibrils in multiple shorter filaments, an indication that a loss of rigidity occurs during the disassembly process. Images reveal a progressive and dramatic separation of the fibril components (protofibrils and building blocks). Very short ensembles of globular features (two or three building units) are further observed as representative features of the final step of the disassembly process over a 1 week treatment with D-carnosine (Figure 6a,b). Figure 6c shows a particular fibril disassembly. Those samples showed only globular features with diameters in the 5−30 nm range (height histograms in Figure 6), indicating that almost complete disassembly can be achieved under these conditions.

α-Crystallin Chaperone Activity. To investigate the effect of destabilizing conditions and the role of carnosine on these, we also tested the chaperone activity for each α-crystallin sample. α-Crystallin in its native form protects β_L-crystallin against aggregation (Figure 7a,e). The ability of the α-crystallin sample, pretreated with 1 M guanidine at 60 °C for 24 h, to protect against this aggregation was remarkably weakened, indicating the formation of no active structures of α-crystallin (Figure 7b). The same sample of α-crystallin, showing a consistent number of fibrillar structures and treated subsequently with carnosine, produces no considerable recovery of the protection against the aggregation of β_L-crystallin (Figure 7c). Finally, the degree of protection of α-crystallin pretreated with carnosine under destabilizing conditions was similar to that of the native form, showing no remarkable reduction in chaperone activity (Figure 7d).

Effects of Carnosine on Rat Lens Organ Cultures. To gain further information about the anti-aggregating activity of carnosine, organ-cultured rat lenses were exposed to denaturing conditions similar to those applied to single crystallins.

Rat lenses dissected by posterior approach were maintained as organ cultures: this model is a valuable tool for investigating the mechanisms of lens homeostasis as well as the mechanisms of cataractogenesis in vitro. Organ-cultured lenses showed no acute leakage of protein into the medium, indicating that they have not been physically damaged during dissection. After 24 h, damaged lenses were eventually discarded. Morphological changes in whole lenses were examined during culture. Not treated, control lenses remained transparent until the end of the treatments.

Groups of at least four lenses were incubated in the presence of guanidine (0.2 or 0.5 M) alone or guanidine with L-carnosine (50 mM) for 24 and 72 h. Treated lenses were checked every day. After treatments, lens opacification was measured by densitometric analysis of pictures acquired with a digital camera. After treatment with 0.2 or 0.5 M guanidine for 24 h, > 90 or > 120% lens opacification, respectively, was observed. After 72 h, there was a further loss of lens transparency of > 120% (0.2 M guanidine) and > 180% (0.5 M guanidine) (Figure 8a).

The protective effect of L-carnosine was tested on other groups of lenses that were treated in the presence of 50 mM L-carnosine, added to the medium 1 h before guanidine. The presence of

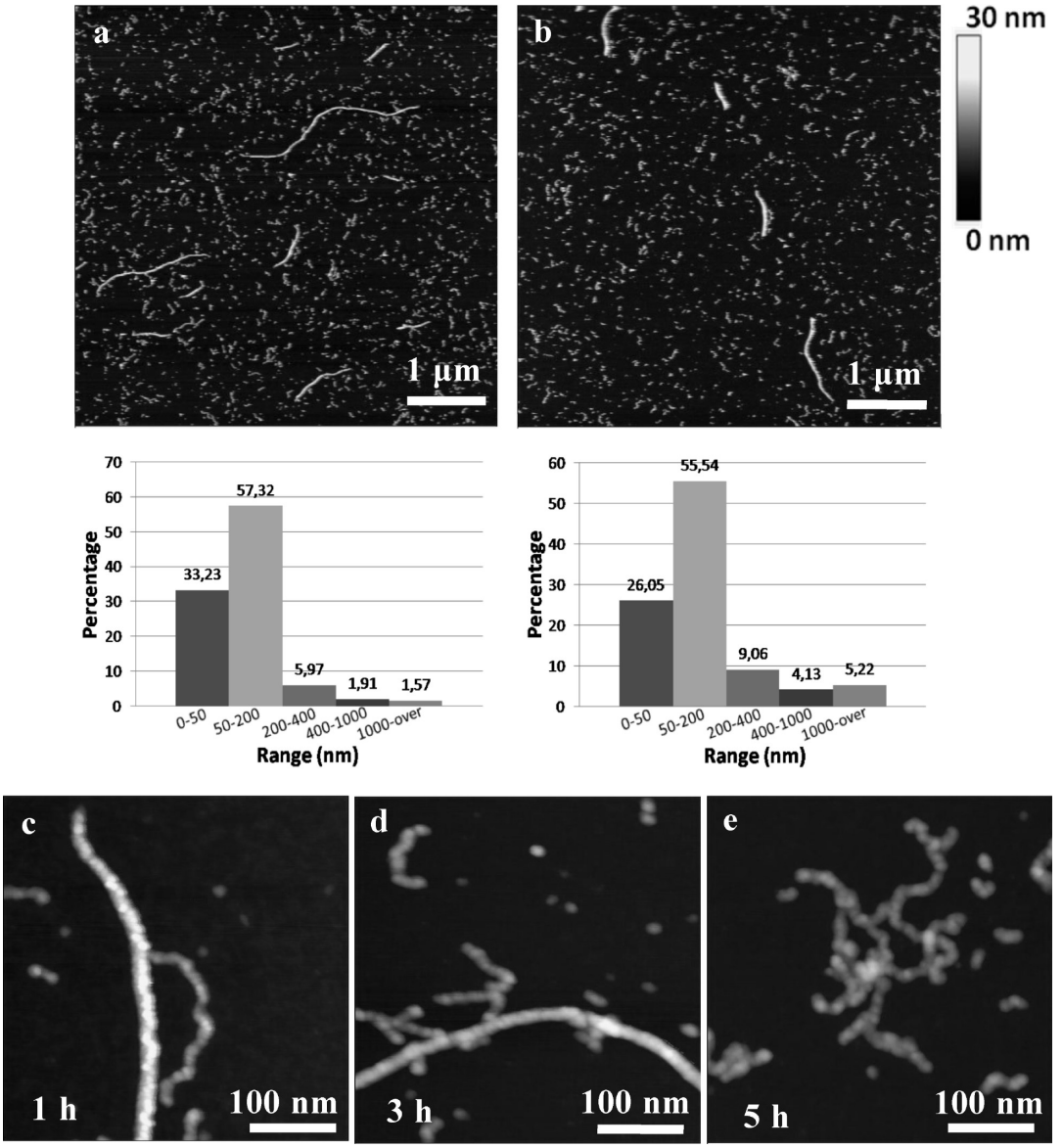

FIGURE 5: SFM images of 10 mg/mL α-crystallin co-incubated at 60 °C for 24 h with 1 M guanidine and treated successively at 25 °C for 1 h with (a) 100 mM D-carnosine and (b) 100 mM L-carnosine and relative statistical distributions of building unit globular structures shown in the images. (c−e) Particular SFM images of 10 mg/mL α-crystallin co-incubated with 1 M guanidine at 60 °C for 24 h and successively treated with 100 mM L-carnosine at 25 °C for 1, 3, and 5 h, respectively.

L-carnosine significantly prevented lens opacification by ~50−60% after either exposure for 24 or 72 h to 0.2 or 0.5 M guanidine (Figure 8a).

To explore the ability of carnosine to restore lens transparency, as it was able to promote disassembly of already formed α-crystallin fibrils, all opaque lenses were placed in new cell culture wells and treated with L-carnosine alone (Figure 8b). After 24 and 48 h, a clear time-dependent recovery of transparency was observed. Lenses previously treated with 0.5 M guanidine with or without L-carnosine showed 50 or 60% recovery after 24 h and 30 or 60% recovery after 48 h, respectively, for this subsequent L-carnosine treatment (Figure 8b). Thus, the L-carnosine capabilities observed in vitro were well confirmed to be effective also on whole organ structures resembling a cataract condition.

DISCUSSION

α-Crystallin is involved in maintaining lens transparency and preventing aggregation of other proteins, being so crucial to avoid cataract formation (*2*, *3*, *47*, *48*). It was demonstrated that denaturant agents associated with heat stress can be used to obtain in vitro α-crystallin self-assembling into amyloid fibrils (*13*, *14*), which would potentially disturb the short-range order of crystallins in the eye lens.

Consequently, molecules that inhibit amyloid aggregation or disaggregate existing amyloid aggregates of this protein can be useful in preventing or controlling the related diseases. It was shown that carnosine has potential biochemical and therapeutic significance (*19*, *21*−*25*). In a previous study, we showed that trehalose inhibits formation of α-crystallin high-molecular weight aggregates (*20*). Moreover, small molecules have been shown to modulate the chaperone activity of αB-crystallin against protein aggregation (*49*).

In this study, we observed that considering α-crystallin alone or the more complex model of lens organ culture, the presence of carnosine prevented fibril formation by denaturant and heat stress and disassembled already formed fibrils, restoring almost completely the lens transparency. Moreover, we show that the self-assembly of α-crystallin into amyloid fibrils determines a loss

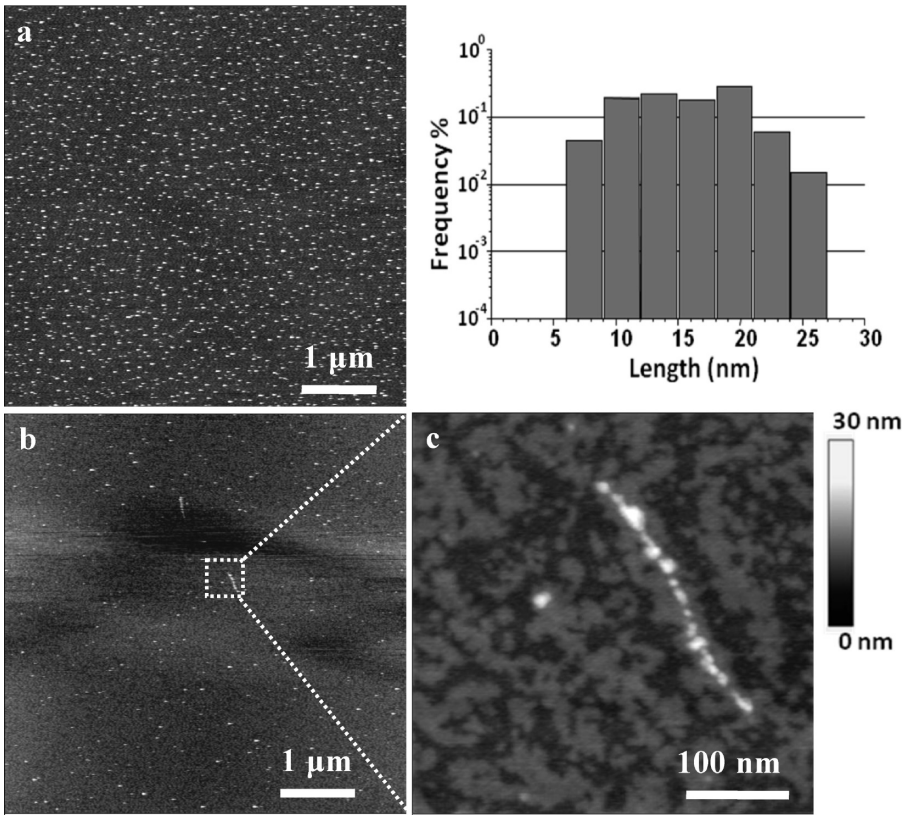

FIGURE 6: SFM images and statistical distribution of globular structures shown in the image in Figure 5a of 10 mg/mL α-crystallin co-incubated at 60 °C for 24 h with 1 M guanidine and successively treated for 1 week with (a) 100 mM L-carnosine or (b) 100 mM D-carnosine. (c) Zoom-in of panel b showing a particular fibril dissolution.

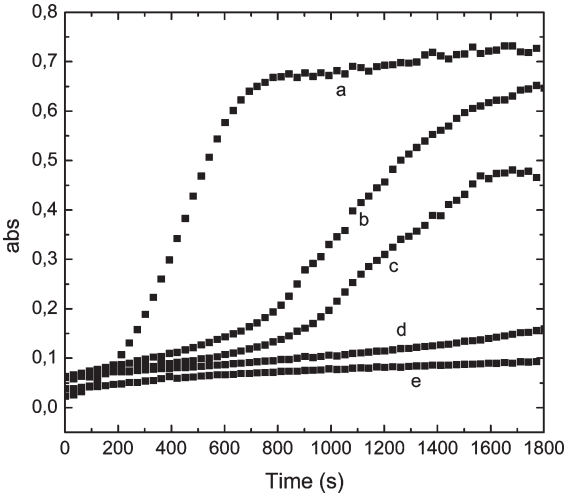

FIGURE 7: Effect of destabilizing conditions and carnosine on the ability of α-crystallin to prevent thermally induced aggregation of *β*-crystallin. The change in the light scattering or turbidity at 400 nm was monitored over time: (a) *β*-crystallin aggregation, (b) *β*-crystallin in the presence of α-crystallin pretreated under destabilizing conditions, (c) *β*-crystallin in the presence of α-crystallin pretreated under destabilizing conditions following treatment with L-carnosine for 5 h, (d) *β*-crystallin in the presence of α-crystallin pretreated under destabilizing conditions with L-carnosine, and (e) *β*-crystallin in presence of native α-crystallin.

of its chaperone activity and that the carnosine protective effect is important for restoring the anti-aggregating activity of α-crystallin.

Under the experimental conditions used in this work, ThT and SFM data show a clear inhibitory effect of α-crystallin fibrillogenesis. The SFM images reveal an aggregation process resembling that already reported in the literature regarding the assembly of globular oligomeric structures (building blocks) followed by an elongation route (*41*); carnosine seems to interfere with fibril growth, preventing fibril extension. In fact, DSC and near-UV CD data show that L- and D-carnosine do not stabilize the protein against guanidine and heat treatment, as demonstrated by the lack of change in the melting temperature, but it does increase the reversibility of thermal melting and reduce the level of formation of protein precipitate under destabilizing conditions. The third and fourth DSC scans produce the disappearance of the endothermic peak and of any event that indicates formation of a precipitate (abrupt decrease in the C_p trace) in the sample containing carnosine; this fact could mean that it failed to prevent the formation of larger soluble unfolded oligomeric species, as also shown in SFM images, but maintained protection against protein precipitation.

Moreover, DSC data argue that the structural precursors of amyloid fibrils are polypeptide chain segments that lack stable structural elements. It is noted that even unfolded chains of polypeptides can retain a significant amount of conformational structural elements, and near-UV CD spectra put in evidence this phenomenon. Other previous observations showed similar mechanisms; for example, myoglobin represents a case of a protein in which amyloid fibril is correlated with the unfolded polypeptide chain (*50*).

By another point of view, we also investigated the disaggregating properties of L- and D-carnosine. We observed, by SFM and ThT results, that carnosine disaggregated α-crystallin amyloid fibrils. In particular, from SFM images and the related statistical analysis, the shorter length distributions of the fibrillar structures indicate an increased susceptibility to breakage, putting in

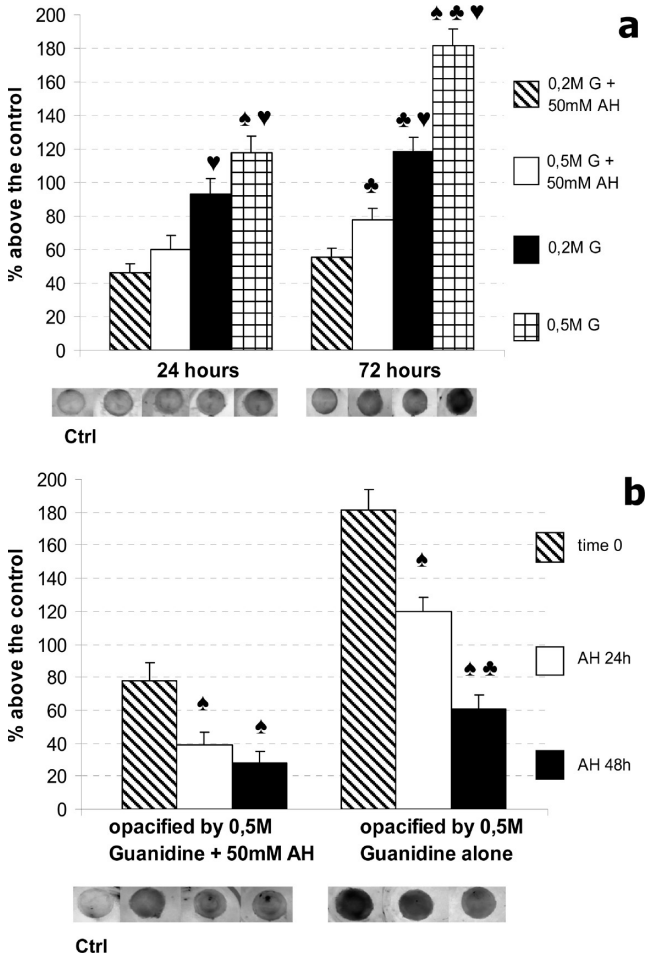

FIGURE 8: (a) Organ-cultured rat lenses treated with guanidine alone or guanidine with L-carnosine. Dose- and time-dependent opacification by guanidine and protection in the presence of L-carnosine: (spade) significant vs 0.2 M guanidine, (club) significant vs 24 h, and (heart) significant vs treatment with L-carnosine. (b) Reversion of the effect of guanidine by treatment with L-carnosine alone. It is particularly evident in those lenses previously opacified with the higher concentration of guanidine alone: (spade) significant vs time 0 and (club) significant vs 24 h.

evidence this disaggregating capacity. In spite of the different histidine moiety, there is no difference in the protective features. Qualitatively, as SFM images reveal, by increasing the incubation time, the fibrils appear sufficiently flexible, extending the probability of fracturing in the "building blocks" (see the linear structure fractured in different globular units in Figure 6c). After 1 week, the images have clearly revealed the presence of a substantial number of short globular structures (8−30 nm).

Interestingly, the inhibitory effect of L- and D-carnosine promoted the almost complete restoration of the chaperone activity loss after denaturant and heat stress. On the contrary, the molecular assembly produced after fracturing of α-crystallin fibrils by carnosine did not restore its activity. It is also interesting to observe that a very similar fibril morphology for α-crystallin can be obtained (i) after inhibition of the fibril growth via co-incubation with carnosine under destabilizing conditions and (ii) after breakage of mature fibrils by addition of carnosine, characteristically observed also in αB-crystallin fibrils obtained via two distinct experimental routes (*14*) and that different chaperone activities are present for these similar morphologies.

These findings, together with DSC observations, could suggest that carnosine, interfering with fibril growth, promotes the formation of large soluble unfolded oligomeric species with chaperone activity.

It is noted in the literature that carnosine derivatives reduce lens opacity in patients with cataracts and canines with age-related cataracts (*30*, *31*, *51*). We therefore performed a study to gain further information about the anti-aggregating activity of carnosine and to explore the ability of carnosine to restore lens transparency; organ-cultured rat lenses were exposed to similar denaturing conditions shown in the experiments in vitro.

Incubation in the presence of guanidine (0.2 or 0.5 M) for 24 and 72 h produced a dense dose- and time-dependent cortical opacification (Figure 8a). This guanidine-induced cataract was partly prevented in the presence of carnosine, added 1 h before guanidine treatments. Moreover, carnosine was shown to be also able to restore transparency of already opacified lenses. Taken together, carnosine treatments showed a visible reversion of the effects of guanidine, either in preventive treatments or as recovery after lens opacification, supporting the notion that lens protein conformational changes, observed also in our study, are strongly associated with lens opacification and can be somehow reversible (Figure 8b).

However, it is worth noting that carnosine is also an antioxidant compound and its ability to protect lenses from opacification can be also attributed to the NO direct quenching effect of carnosine (*52*) or inhibition of iNOS induction under stressing conditions (*53*). Indeed, high levels of iNOS mRNA and iNOS protein expression have been found in cataractous lenses, and oral administration of aminoguanidine, a specific iNOS inhibitor, markedly suppressed or prevented lens opacification (*54*, *55*). Carnosine is also present in the eye lenses at a high level (*56*, *57*); therefore, our result supports the hypothesis that a possible decrease during aging, as it is known in the muscle (*58*), could contribute to age-related cataractogenesis.

Several events such as thermal and/or chemical insults contribute to the determination of protein aggregation and fibrillogenesis; conformational changes induced under destabilizing conditions, as in the presence of guanidine and heat stress, are responsible for these aberrant interprotein interactions. The inhibition of fibril formation and/or disaggregation of fibrillar aggregates can contribute in part to reversing damage caused by protein aggregation.

In conclusion, in this study, we observed that considering α-crystallin alone or the more complex model of lens organ culture, the presence of carnosine prevents fibril formation, maintains chaperone activity, and disassembles already formed fibrils, restoring almost completely lens transparency. Moreover, because of its resistance to carnosinases, D-carnosine can be a valuable therapeutic tool.

It should also be noted that the effects on the whole lens underscore the effectiveness of carnosine on a wide range of proteins and therefore its nonspecific action. Moreover, it appears that carnosine exerts its protecting features irrespective of the type of stress (*25*). The anti-aggregating activity on a specific protein like α-crystallin alone resembles only partially what carnosine can do with respect to, for example, different protein interactions and particularly to highly ordered protein structures. These are typically related to a set of proteins that has been found to convert readily into amyloid fibrils, thus stimulating interest in those molecules that, like carnosine, can effect the changes from the native functional state and the formation of amyloid fibrils associated with a number of disorders linked to the deposition of misfolded proteins.

ACKNOWLEDGMENT

We thank Flamma s.p.a. for D-carnosine.

REFERENCES

1. Bloemendal, H. (1981) in Molecular and Cellular Biology of the Eye Lens , Wiley, New York.
2. Horwitz, J. (1992) α-Crystallin can function as a molecular chaperone. *Proc. Natl. Acad. Sci. U.S.A. 89*, 10449–10453.
3. Horwitz, J. (2003) α-Crystallin. *Exp. Eye Res. 76*, 145–153.
4. Harding, J. J. (2002) Viewing molecular mechanisms of ageing through a lens. *Ageing Res. Rev. 1*, 465–479.
5. Derham, B. K., and Harding, J. J. (2002) Effects of modifications of α-crystallin on its chaperone and other properties. *Biochem. J. 364*, 711–717.
6. Spector, A., Li, L. K., Augusteyn, R. C., Schneider, A., and Freund, T. (1971) α-Crystallin. The isolation and characterization of distinct macromolecular fractions. *Biochem. J. 124*, 337–343.
7. Liang, J. J.-N., and Akhtar, N. J. (2000) Human lens high-molecular-weight α-crystallin aggregates. *Biochem. Biophys. Res. Commun. 275*, 354–359.
8. Fujii, N., Awakura, M., Takemoto, L., Inomata, M., Tarata, T., Fujii, N., and Saito, T. (2003) Characterization of αA-crystallin from high molecular weight aggregates in the normal human lens. *Mol. Vision 9*, 315–322.
9. Sunde, M., and Blake, C. C. (1998) From the globular to the fibrous state: Protein structure and structural conversion in amyloid formation. *Q. Rev. Biophys. 31*, 1–39.
10. Van Boekel, M. A., Hoogakker, S. E., Harding, J. J., and De Jong, W. W. (1996) The infuence of some post-translational modifications on the chaperone-like activity of α-crystallin. *Ophthalmic Res. 28*, 32–38.
11. Pande, A., Pande, J., Asherie, N., Lomakin, A., Ogun, O., King, J. A., Lubsen, N. H., Walton, D., and Benedek, G. B. (2000) Crystal cataracts: Human genetic cataracts caused by protein crystallization. *Proc. Natl. Acad. Sci. U.S.A. 97*, 1993–1998.
12. Harding, J. J. (1998) Cataract, Alzheimer's disease, and other conformational diseases. *Curr. Opin. Ophthalmol. 9*, 10–13.
13. Meehan, S., Berry, Y., Luisi, B., Dobson, C. M., Carver, J. A., and MacPhee, C. E. (2004) Amyloid fibril formation by lens crystallin proteins and its implications for cataract formation. *J. Biol. Chem. 279*, 3413–3419.
14. Meehan, S., Knowles, T. P. J., Baldwin, A. J., Smith, J. F., Squires, A. M., Clements, P., Treweek, T. M., Ecroyd, H., Tartaglia, G. G., Vendruscolo, M., MacPhee, C. E., Dobson, C. M., and Carver, J. A. (2007) Characterisation of amyloid fibril formation by small heat-shock chaperone proteins human αA-, αB- and R120G αB-crystallin. *J. Mol. Biol. 372*, 470–484.
15. Tanaka, M., Machida, Y., Niu, S., Ikeda, T., Jana, N. R., Doi, H., Kurosawa, M., Nekooki, M., and Nukina, N. (2004) Trehalose alleviates polyglutamine-mediated pathology in a mouse model of Huntington disease. *Nat. Med. 10*, 148–154.
16. Arora, A., Ha, C., and Park, C. B. (2004) Inhibition of insulin amyloid formation by small stress molecules. *FEBS Lett. 564*, 121–125.
17. Akashi, K., Miyake, C., and Yokota, A. (2001) Citrulline, a novel compatible solute in drought-tolerant wild watermelon leaves, is an efficient hydroxyl radical scavenger. *FEBS Lett. 508*, 438–442.
18. Tanaka, M., Machida, Y., and Nukina, N. J. (2005) A novel therapeutic strategy for polyglutamine diseases by stabilizing aggregation-prone proteins with small molecules. *Mol. Med. 83*, 343–352.
19. Yan, H., and Harding, J. J. (2006) Carnosine inhibits modifications and decreased molecular chaperone activity of lens α-crystallin induced by ribose and fructose 6-phosphate. *Mol. Vision 12*, 205–214.
20. Attanasio, F., Cascio, C., Fisichella, S., Nicoletti, V. G., Pignataro, B., Savarino, A., and Rizzarelli, E. (2007) Trehalose effects on α-crystallin aggregates. *Biochem. Biophys. Res. Commun. 354*, 899–905.
21. McFarland, G. A., and Holliday, R. (1994) Retardation of the senescence of cultured human diploid fibroblasts by carnosine. *Exp. Cell Res. 212*, 167–175.
22. Gariballa, S. E., and Sinclair, A. J. (2000) Carnosine: Physiological properties and therapeutic potential. *Age Ageing 29*, 207–210.
23. Hipkiss, A. R., Michaelis, J., and Syrris, P. (1995) Non-enzymatic glycosylation of the dipeptide L-carnosine, a potential anti-protein-cross-linking agent. *FEBS Lett. 371*, 81–85.
24. Brownson, C., and Hipkiss, A. R. (2000) Carnosine reacts with a glycated protein. *Free Radical Biol. Med. 28*, 1564–1570.
25. Seidler, N. W., Yeargans, G. S., and Morgan, T. G. (2004) Carnosine disaggregates glycated α-crystallin: An in vitro study. *Arch. Biochem. Biophys. 427*, 110–115.
26. Kang, J. H., Kim, K. S., Choi, S. Y., Kwon, H. Y., Won, M. H., and Kang, T. C. (2002) Protective effects of carnosine, homocarnosine and anserine against peroxyl radical-mediated Cu,Zn-superoxide dismutase modification. *Biochim. Biophys. Acta 1570*, 89–96.
27. Yan, H., and Harding, J. J. (2005) Carnosine protects against the inactivation of esterase induced by glycation and steroid. *Biochim. Biophys. Acta 1741*, 120–126.
28. Yan, H., and Harding, J. J. (2006) Protective effects of carnosine against the inactivation of ezymes induced by glycation and steroid: Relevance to cataract. *Am. J. Ophthalmol. 139* (Suppl.), S55.
29. Hipkiss, A. R., Presto, J. E., Himswoth, D. T., Worthington, V. C., and Abbot, N. J. (1997) Protective effects of carnosine against malondialdehyde-induced toxicity towards cultured rat brain endothelial cells. *Neurosci. Lett. 238*, 135–138.
30. Babizhayev, M. A., Guiotto, A., and Kasus-Jacobi, A. (2009) N-Acetylcarnosine and histidyl-hydrazide are potent agents for multi-targeted ophthalmic therapy of senile cataracts and diabetic ocular complications. *J. Drug Targeting 17*, 36–63.
31. Babizhayev, M. A., Deyev, A. I., Yermakova, V. N., Remenshchikov, V. V., and Bours, J. (2006) Revival of lens transparency with N-acetylcarnosine. *Curr. Drug Ther. 1*, 91–116.
32. Boldyrev, A., Bulygina, E., Leinsoo, T., Tsubone, I. P. S., and Abe, H. (2000) Protection of neuronal cells against reactive oxygen species by carnosine and related compounds. *Comp. Biochem. Physiol., Part B: Biochem. Mol. Biol. 127*, 443–446.
33. Aldini, G., Canevotti, R., and Negrisoli, G. Compositions containing D-carnosine. Patent WO 2005/120543.
34. Pignataro, B., Chi, L. F., Gao, S., Anczykowski, B., Niemeyer, C. M., Adler, M., Blohm, D., and Fuchs, H. (2002) Dynamic scanning force microscopy study of self-assembled DNA-protein oligomers. *Appl. Phys. A: Mater. Sci. Process. 74*, 447–452.
35. Pignataro, B., Sardone, L., and Marletta, G. (2003) Dynamic scanning force microscopy investigation of nanostructured spiral-like domains in Langmuir-Blodgett monolayers. *Nanotechnology 14*, 245–249.
36. García, J., Martinez, L., Briceño-Valero, J. M., and Schilling C. H. (1997) Dimensional Metrology of Nanometric Spherical Particles using AFM: I. Model Development. *Probe Microsc. 1*, 107–116.
37. Vesenka, J., Tang, C. L., Guthold, M., Keller, D., Delaine, E., and Bustamante, C. (1992) A substrate preparation for imaging biomolecules with the scanning force microscope. *Ultramicroscopy 42−44*, 1243–1249.
38. Naiki, H., Higuchi, K., Hosokawa, M., and Takeda, T. (1989) Fluorometric determination of amyloid fibrils in vitro using the fluorescent dye, thioflavine T. *Anal. Biochem. 177*, 244–249.
39. LeVine, H.III (1999) Quantification of β-sheet amyloid fibril structures with thioflavin T. *Methods Enzymol. 309*, 274–284.
40. Burgio, M. R., Bennett, P. M., and Koretz, J. F. (2001) Heat induced quaternary transitions in hetero- and homo-polymers of α-crystallin. *Mol. Vision 7*, 228–233.
41. Blackley, H. K., Sanders, G. H., Davies, M. C., Roberts, C. J., Tendler, S. J., and Wilkinson, M. J. (2000) In-situ atomic force microscopy study of β-amyloid fibrillization. *J. Mol. Biol. 298*, 833–840.
42. Lee, J. C., and Timasheff, S. N. (1974) Partial specific volumes and interactions with solvent components of proteins in guanidine hydrochloride. *Biochemistry 13*, 251–265.
43. Makhatadze, G. I., and Privalov, P. L. (1992) Protein interactions with urea and guanidinium chloride. A calorimetric study. *J. Mol. Biol. 226*, 491–505.
44. Horwitz, J. (1976) Some properties of the low molecular weight α-crystallin from normal human lens: Comparison with bovine lens. *Exp. Eye Res. 23*, 471–481.
45. Horwitz, J., Strickland, E. H., and Billups, C. (1969) Analysis of the vibrational structure in the near-ultraviolet circular dichroism and absorption spectra of phenylalanine and its derivatives. *J. Am. Chem. Soc. 91*, 184–190.
46. Horwitz, J., Strickland, E. H., and Billups, C. (1970) Analysis of the vibrational structure in the near-ultraviolet circular dichroism and absorption spectra of tyrosine derivatives and ribonuclease A at 77 K. *J. Am. Chem. Soc. 92*, 2119–2129.
47. Derham, B. K., and Harding, J. J. (1999) α-Crystallin as a molecular chaperone. *Prog. Retinal Eye Res. 18*, 463–509.
48. Sun, Y., and MacRae, T. H. (2005) The small heat shock proteins and their role in human disease. *FEBS J. 272*, 2613–2627.

49. Heath, E., and Carver, J. A. (2008) The effect of small molecules in modulating the chaperone activity of αB-crystallin against ordered and disordered protein aggregation. *FEBS J. 275*, 935–947.
50. Fändrich, M., Forge, V., Buder, K., Kittler, M., Dobson, C. M., and Diekmann, S. (2005) Myoglobin forms amyloid fibrils by association of unfolded polipeptide segments. *Proc. Natl. Acad. Sci. U.S.A. 100*, 15463–15468.
51. Babizhayev, M. A., Deyev, A. I., Yermakova, V. N., Semiletov, Y. A., Davydova, N. G., Doroshenko, V. S., Zhukotskii, A. V., and Goldman, I. M. (2002) Efficacy of N-acetylcarnosine in treatments of cataracts. *Drugs R&D 3*, 87–103.
52. Nicoletti, V. G., Santoro, A. M., Grasso, G., Vagliasindi L. I., Giuffrida, M. L., Cuppari, C., Purrello, V. S., Giuffrida-Stella, A. M., and Rizzarelli, E. (2007) Carnosine interaction with nitric oxide and astroglial cell protection. *J. Neurosci. Res. 85*, 2239–2245.
53. Calabrese, V., Colombrita, C., Guagliano, E., Sapienza, M., Ravagna, A., Cardile, V., Scapagnini, G., Santoro, A. M., Mangiameli, A., Butterfield, D. A., Giuffrida Stella, A. M., and Rizzarelli, E. (2005) Protective Effect of Carnosine During Nitrosative Stress in Astroglial Cell Cultures. *Neurochem. Res. 30*, 797–807.
54. Inomata, M., Hayashi, M., Shumiya, S., Kawashima, S., and Ito, Y. (2001) Involvement of inducible nitric oxide synthase in cataract formation in Shumiya cataract rat (SCR). *Curr. Eye Res. 23*, 307–311.
55. Nagai, N., Liu, Y., Fukuhata, T., and Ito, Y. (2006) Inhibitors of Inducible Nitric Oxide Synthase Prevent Damage to Human Lens Epithelial Cells Induced by Interferon-γ and Lipopolysaccharide. *Biol. Pharm. Bull. 29*, 2077–2081.
56. Babizhayev, M. A., Yermakova, V. N., Sakina, N. L., Evstigneeva, R. P., Rozhkova, E. A., and Zheltukhina, G. A. (1996) Nα-Acetylcarnosine is a prodrug of L-carnosine in ophthalmic application as antioxidant. *Clin. Chim. Acta 254*, 1–21.
57. Jay, J., Miller, D. J., Morrison, J. D., and O'Dowd, J. J. (1990) Histidyl derivates in rabbit lens and their diminution in human cataract. Meeting Abstracts of the Journal of Physiology of London , Proceedings Supplement, Vol. 420, p 155.
58. Stuerenburg, H. J. (2000) The roles of carnosine in aging of skeletal muscle and in neuromuscular diseases. *Biochemistry (Moscow, Russ. Fed.) 65*, 862–865.